doi:10.1038/nature11022

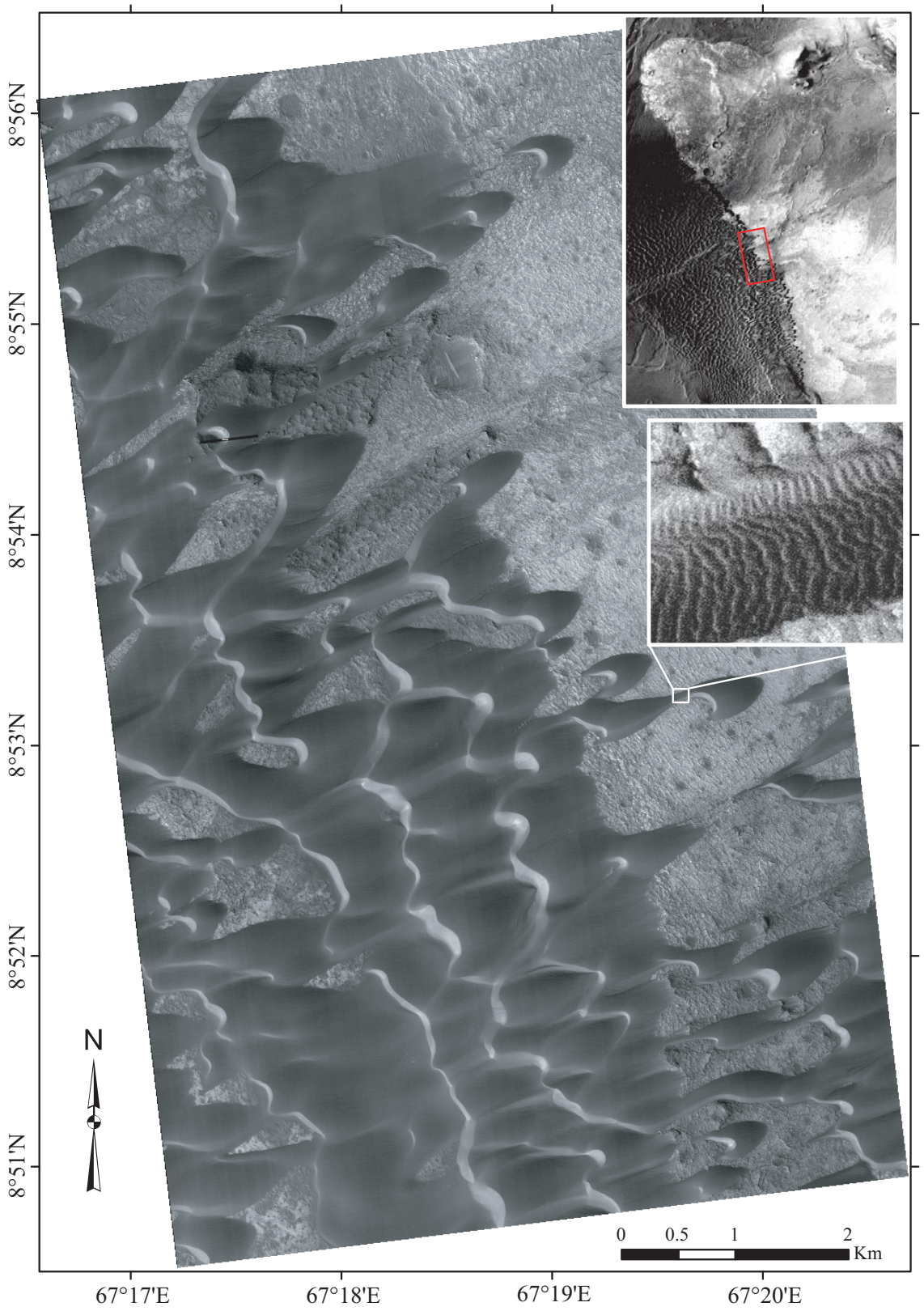

Supplementary Figure 1/ HiRISE image PSP_004339_1890 showing the Nili Patera dune field study area where images *T*1 and *T*2 overlap. Upper inset shows location of this area (red box) with respect to the entire dune field in CTX image P04_002427_1888_XI_08N292W. Lower inset is a close-up view of one of the dunes, showing the rippled surface.

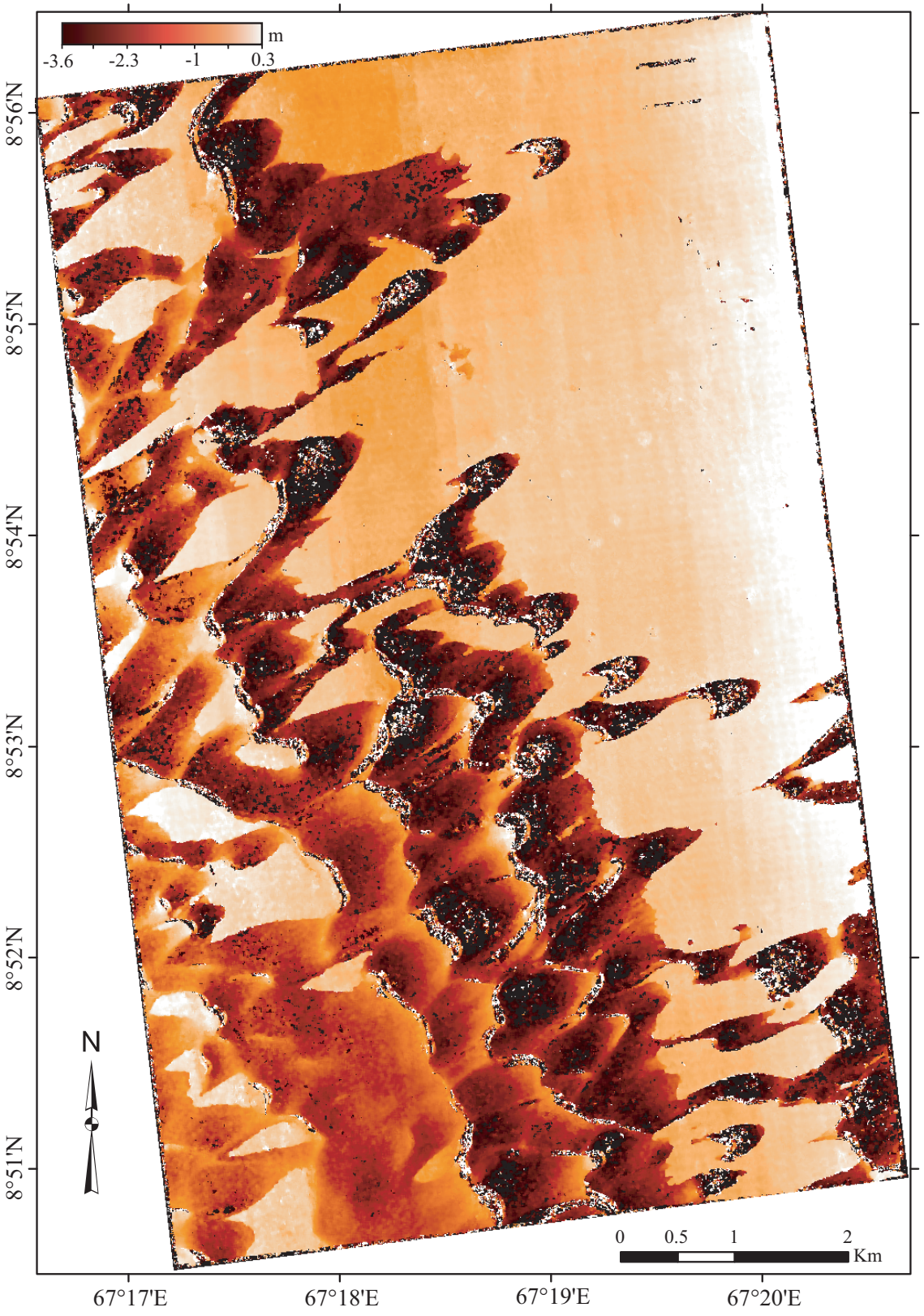

Supplementary Figure 2/ East/West component of the *T*1/*T*2 correlation. Displacements are positive toward the East. Ripple displacements are measured up to around 3.6 m. Above this value, the correlation mostly fails as the ripple pattern changes too much between *T*1 and *T*2 (shown as white pixels).

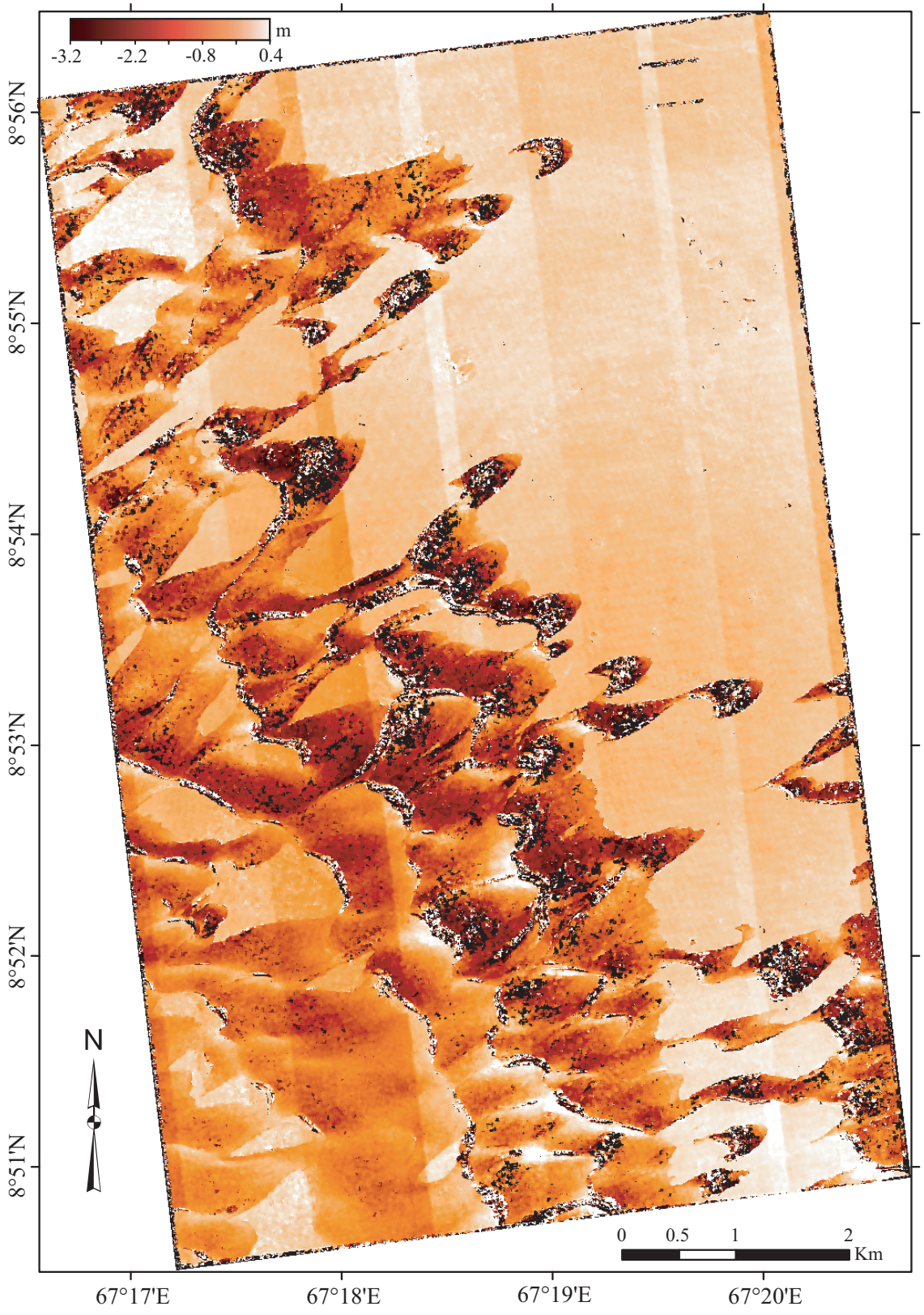

Supplementary Figure 3/ North/South component of the *T*1/*T*2 correlation. Displacements are positive toward the north. Toward the south, values up to around 3.2 m are measured. Above this value, the correlation mostly fails as the ripple pattern changes too much between *T*1 and *T*2 (shown as white pixels). Along-track stripes are due to CCD array misalignment residual, with an amplitude of more than 1 pixel for the most misaligned CCD.

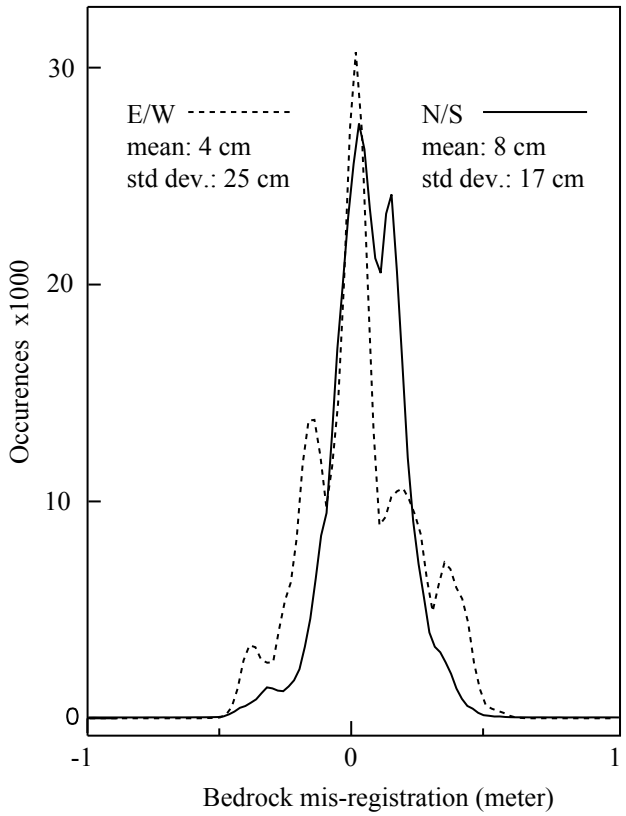

Supplementry Figure 4/ Histograms of displacement (in East/West and North/South directions) measured on the bedrock only. These measurements give an indication on the *T*1 and *T*2 registration quality and the minimum displacement that can potentially be measured.

Methods

Background

Recent advances in image modeling and processing[12] permit the measurement of relative displacements between images to the sub-pixel level. Methodological improvements in this field have been implemented in the software package Co-registration of Optically Sensed Images and Correlation (COSI-Corr)[31]. Correlation requires unambiguous discrimination features. This technique has been successfully employed to measure displacements on Earth, including fault offsets, ice flows, landslides, and sand dune migration[12,13,32,33]

Data set

A total of four HiRISE images were used to measure ripple migration rates (SOM Table 1). Two images were used to extract the topography (*S*1 and *S*2), and the others used to measure ripple migration (*T*1 and *T*2). Images *T*2 and *S*1 were also used to assess overall dune displacement.

SOM Table 1: HiRISE Images Used For Analysis

Image ID	ID	Roll Angle (°)	L_s(°)	Date Acquired	ΔTime (Days)
PSP_004339_1890	*T*1	-0.353	268	6/30/07	0
PSP_005684_1890	*T*2	-4.001	330	10/13/07	105
ESP_017762_1890	*S*1	25.269	89	5/11/10	1046
ESP_018039_1890	*S*2	-4.98	99	6/2/10	1068

ID = Abbreviated identification used in the text; roll angle is the off-nadir pointing of the spacecraft (which is equivalent to the HiRISE boresight), with positive values toward the west and negative toward the east; L_s is the areocentric longitude of Mars's orbit around the Sun, with L_s = 0° corresponding to the beginning of northern spring and southern autumn. All images have a resampled pixel scale of 25cm.

Digital Elevation Model extraction

Images *S1* and *S*2 were specifically acquired for stereo-photogrammetry. They were taken 22 days apart in 2010 with a viewing angle difference of 32.9 degrees. The Digital Elevation Model (DEM) extraction was carried out at the HiRISE Operations Center at University of Arizona using the United States Geological Survey (USGS) recommended procedure[34] that incorporates the Integrated Software for Imagers and Spectrometers (ISIS) image processing package[35] and SOCET SET stereo software[36]. The extracted DEM had a post-spacing of 1m and was manually edited in some places. At these locations the DEM extraction failed mainly because of textureless areas, especially on the dunes' lee side. The two images were subsequently orthorectified on a ~25cm resolution grid.

HiRISE imagery is subject to jitter that, if not corrected, may introduce distortions in the DEM[37]. The University of Arizona developed a procedure to remove jitter distortions from HiRISE images prior to further processing[38]. However, corrections are only applied if jitter amplitude is larger than 1-2 pixels, which was not the case with the *S*1 and *S*2 images. Notice that we neglect possible topographic changes between these two images. This assumption is discussed and justified below.

Dune height extraction

The first step for determining dune height based on the DEM was to define regions of bedrock. This was done by setting an amplitude threshold on the ripple displacement map (Fig. 1a). The bedrock area was then adjusted from visual inspection of the images (the

sand being darker than the bedrock) in areas close to the dunes, and in areas for which bedrock mis-registration was above the threshold. The bedrock topography beneath the dune field was then extrapolated using a thin plate spline interpolation[39]. In practice, the bedrock contained too many points for the thin plate spline algorithm to ingest. Therefore, around 5000 points, evenly spread, were extracted from the bedrock areas. Additional points were extracted around the dune footprints. The interpolated bedrock topography beneath the dunes was then replaced in the main DEM. The resulting bedrock topography model (SOM Movie 2) was then subtracted from the DEM to yield the dune height map shown in Fig. 1c.

Image processing:

Images *T*1 and *T*2 were used to evaluate ripple migration. These were acquired 105 days apart in 2007, with a difference in viewing angle of 4.0 degrees. Both images have a resampled ground resolution of 25cm. Before correlation, the images went through a two step process using ISIS and COSI-Corr.

Both images were supplied by the USGS in a radiometrically and geometrically calibrated format ("balanced cubes") in the form of 10 stripes corresponding to the 10 CCD arrays in the broadband "red" channel[14,37,40]. Camera jitter was estimated by the University of Arizona using standard procedures[38]. The stripes were then processed using ISIS and the USGS procedure (hijit4socet script). This process stitched the stripes together, while correcting for the jitter estimate and accounting for the camera geometry, outputting an image as if it was acquired by an ideal, distortion-free camera. The images

were then formatted into a SOCET SET readable format with the ancillary data (e.g., ephemeris, camera geometry) extracted from the SPICE (ancillary data) kernels[41].

The images and the extracted ancillary data were plugged into COSI-Corr[12] rather than into SOCET SET to take advantage of the optimized co-registration feature in order to finely register images before correlation. Fifty tie-points were selected between image *T*1 and orthorectified image *S*1. The tie-points were evenly spread over the images and were located in bedrock areas away from the dunes. The tie-points were optimized using COSI-Corr using a window size of 256x256 pixels. The resulting average mis-registration between the two images at the tie-point locations was less than 1/100th of a pixel with a standard deviation of 0.46 pixel (11.5cm) in the East/West direction and 0.58 pixel (14.5cm) in the North/South direction. Image *T1* was then orthorectified with COSI-Corr on a 25cm grid, using the ancillary data, the optimized set of tie-points, and the DEM previously extracted. Image *T*2 was then co-registered to orthorectified image *T*1. The same procedure as above was applied with similar co-registration accuracy.

Orthorectified images *T*1 and *T*2 were correlated with COSI-Corr using a sliding correlation window of 70x70 pixels (17.5x17.5m) and a step of 16 pixels (4m). The displacement maps obtained are presented in SOM Fig. 2 and SOM Fig. 3 and represent respectively the East/West (positive eastward) and North/South (positive northward) components of the displacement field. SOM Fig. 4 presents the histogram of the entire bedrock mis-registration. The average ripple displacement is about 2.5m, with measureable peaks at 4m. In the North/South displacement map, CCD artifacts can be

seen that are residuals of the camera geometry model. Their amplitude varies from negligible up to ~0.35m. Theses artifacts are also found in the East/West direction but are overprinted by ripple displacements. The amplitude displacement map (Fig.1) represents the norm of the displacement from the East/West and North/South components.

Elevation error ambiguity

As observed in Fig. 1-2, the displacements are highly correlated to dune topography, such that topographic error could be considered a factor. We show that this is not the case because:

1) Given the baseline and height ratio of the two images, an error of 30m in elevation would be necessary to produce 2.5m of displacement. This is highly unlikely as the vertical DTM accuracy is a few tens of centimeters for a SOCET SET matching accuracy of one pixel. The dunes themselves have a height ranging from a few meters to around 50m.

2) Displacements visually estimated in previous work[3] from images *T*1 and *T*2 compare well with our results.

3) The displacement maps, which are in East/West and North/South directions, were projected onto the epipolar and perpendicular-epipolar directions that are defined from the image acquisition geometries. All parallax related displacements are therefore projected onto the epipolar direction, in particular the topographic residuals. If the ripple displacements measurements were only due to topographic error, they would be entirely in the epipolar direction. However, the perpendicular epipolar direction displays ripple displacements, invalidating the hypothesis possibility of parallax error.

Errors due to topographic changes between *S*1 and *S*2

This study assumes that the dunes and ripples remain static in the 22 days between *S*1 and *S*2, such that an accurate DEM is derived. This was verified as follows:

1) Stereoscopic error induced by ripple migration

SOCET SET matches textured surfaces for topographic extraction. The ripple pattern is used during the matching to infer the dune heights. We determined the error made on the DEM if the ripples moved during the 22 day span between *S*1 and *S*2.

Taking the average and maximum displacements of 2.5 and 4m in the 105 days between *T*1 and *T*2 implies that motion in 22 days would be 0.52m and 0.83m, inducing an error on the dune topography of 0.8m and 1.29m respectively. This elevation error would in turn causes a displacement map bias of about 6 and 11cm, respectively. This value (a few centimeters) is small enough relative to the measured displacements (a few meters) to be negligible. In addition, no ripple displacement could be detected visually between the stereo images, suggesting an even smaller topographic error.

2) Error due to the assumption of static dune topography

With an average of 2.5m ripple displacement in 105 days, the dunes themselves may well have moved in the three year period between the acquisition of the images for correlation (*T*1 and *T*2) and the ones for DEM extraction (*S1* and *S*2), making the assumption of static dune topography incorrect. Dune fronts were visually checked between the 941 day

time separation between *T*2 and *S*1. Obviously the images could not be correlated as the ripples pattern changed entirely in three years. However, taking advantage of the good image registration between *T*2 and *S*1, up to 2-3m of dune migration was manually measured in some cases (SOM Animation 2), whereas other dunes were static. According to the DEM, the slope of the dunes' stoss sides in the "axial" direction is in the range 4-8°. Assuming a dune displacement of 3m, a stoss slope of 6°, and a static morphology and height over this time scale, an error of around 30cm in elevation would be introduced. As discussed above, an elevation error of 1m induces a ~ 10cm bias in the displacement maps. Consequently, a 30cm error in elevation would introduce a displacement bias at the centimeter scale, which can be neglected in view of the measured ripple displacements.

Estimates of the mean ripple height

The ripple pattern is clearly seen in the HiRISE images as they form alternating thin bright bands between thick dark bands, implying asymmetric slopes analogous to ripples on Earth[42,43]. The DEM has insufficient resolution to resolve the ripple topography. The mean height of the crest of the ripples (measured with respect to the elevation of the trough between the ripples) can nonetheless be estimated to 40cm, based on the following two approaches.

We measured 5 ripple trains consisting of 9-13 ripples each. These had average wavelengths ranging from 3.6m to 5.3m. The mean value is estimated to 4.6±0.09m. Assuming that the Nili ripples have height to wavelength ratios like those of many

terrestrial aeolian ripples[42,43] and "transverse aeolian ridges" elsewhere on Mars[43], values are ~1:10. Therefore, assuming a typical wavelength on the order of 4.5m, implies that the ripples are ~45±9cm high. The uncertainty on the height to wavelength ratio is difficult to assess and not taken into account in this estimate.

In some areas the shape of ripples that are in contact with the bedrock at the dune base can be clearly delineated against the bedrock. Using the local slope of the dune and the profiles of the ripple projections on the bedrock, an estimate of the ripple height was obtained. On average, from 7 measurements at 2 different sites the height was estimated at 35±3cm. Based on these two approaches, we estimate the ripple height at the crest, as 40± 9cm.

The mean height, h_r, of the ripples, which is the quantity that determines the reptation sand flux, depends on the crest height but also on the ripple geometry. If the ripples are assumed sinusoidal or triangular[44] makes no difference as in both cases the mean height is actually half the crest height. The ripple geometry need only be considered if there is a significant dissymmetry of concavity between the convex and concave portions of the ripple profile. In absence of constraints on ripple geometry we assume that this factor might result in an additional 10% source of relative uncertainty. Altogether we estimate the relative uncertainly on the mean ripple height as on the order of 30%, so h_r=20±6cm.

Relation between dune celerity and sand flux in steady-state

A migrating dune that maintains its shape and volume is considered at steady-state. Conservation of mass for such a dune writes in 1-*D* as

$$\rho_s \partial h_D/\partial t = -c\ \rho_s \partial h_D/\partial x = -\quad q$$

where ρ_s is the sand density, h_D is local dune height, t is the time, c is the dune migration rate, x is the transport direction, and $\boldsymbol{q}(x, t)$ is the mass sand flux[15]. The dune slope from the upwind edge to the crest should be nearly constant. Integrating the above equation therefore gives

$$c\rho_s h_D = q$$

Therefore, the flux increases with increasing elevation on a dune surface. The total flux is the combined saltation (q_s) and reptation (q_r) fluxes. The ratio, α between the two fluxes depends on the local conditions[17,18]; we can write:

$$c\rho_s h_D = (1+\alpha) q_r$$

Considering the ripple migration-induced sand flux equal to the reptation sand flux. Hence,

$$q_r = h_r d_r \rho_s / t$$

with h_r the mean ripple height, d_r the ripple displacement, and t the time interval. Hence,

$$c=(1+\alpha)h_r d_r/h_D t$$

For a constant mean ripple height h_r, a dune at steady state requires that d_r/h_D be constant. This linear relationship between d_r and h_D is observed in the measurements (Fig. 2), and we found no evidence for systematic spatial variation of ripple size (h_r is therefore assumed constant).

Because dune migration rate and flux derived from ripple displacement are proportional to the ripple height, deviation from the assumed constant h_r of 20cm is the greatest contributor to the uncertainty. With the height measurement techniques varying by ±6cm (see above), the reptation flux and the dune migration rates derived from ripple migration rates have an uncertainty of ~30%.

Resolution of Technique

The minimum derived dune migration contributed by reptation flux depends on the minimum ripple displacement that can be measured, or $c \sim d_r h_r/h_D t$. In practice, with HiRISE images, the COSI-Corr correlator has a displacement detection capability of around 3cm, give or take a few centimeters depending on the scene texture. The detection threshold is usually assessed by looking at the standard deviation of the measured displacements over a patch of supposedly uniform displacement. In Nili Patera this estimation is hard to make on the dunes themselves, as ripple displacements increase or decrease along the dune slope and are not uniform on any given patch. We therefore

estimated the measurement resolution on the bedrock, which is around 4cm (SOM Fig. 4). Although the resolution could be different on the bedrock and on the dunes, the texture on both surfaces contain enough high frequencies to expect a similar measurement resolution. The smallest displacements are around 20cm, so all measurements are well above this limit. Notice, however, the difference between the resolution and the absolute accuracy of the measurements which may be biased by local mis-registration. The ripple-derived dune migration rate is $c \sim d_r h_r / h_D t$. With a 20cm mean ripple height, the minimum detectable dune migration rate over 105 days is therefore $8 \times 10^{-3} / h_D$ m. Dune heights range from the maximum brink value of 61.5m to the minimum 0.5m used in the calculation, translating into a threshold over 105 days of 1.3×10^{-4} to 1.6×10^{-2}m, or, over an Earth year, 4.5×10^{-4} to 5.5×10^{-2}m, respectively. Therefore, there is a range of thresholds, depending on the local dune height. However, the dropping of the histogram in Fig. 3 at values < 0.1m is not because of this limitation, since, as just described, all displacements were above the resolution limit. In other words, Fig. 3 represents all ripple-derived dune migration rates.

Calculation of Abrasion Rate

Abrasion susceptibility (S_a) is defined as the ratio of the mass lost from a rock surface to that of the impacting sand and has been measured for a range of conditions and compositions in the laboratory[25]. At fluid threshold, S_a for basalt grains hitting basalt rocks at 20m s^{-1} is ~2×10^{-4}. However, as discussed in the main text, sand fluxes on Mars are sustained at impact threshold conditions with wind and particle impact speeds about

10% that at fluid threshold, equivalent to typical terrestrial values[24]. Abrasion susceptibility is proportional to grain kinetic energy[25], such that S_a should be ~2x10^{-6} at impact threshold. Because the density of both materials are the same, the abrasion susceptibility is also the ratio of rock volume loss to the volume of impacting sand. The flux of sand that we calculate is that passing through a vertical cross section and this must be converted to the flux hitting a surface ranging in slope (θ) from flat ground (θ = 0°) to a vertical face (θ = 90°). We can therefore consider the abrasion rate equal to $(S_a Q_i/z)(\alpha\cos\theta + \sin\theta)$, where Q_i is the interdune sand flux and α is the ratio of saltation height to descending path length. The mean trajectory height (z) on Mars, considering both reptating and saltating grains, has been calculated as ~10 to a few 10s of centimeters, with the exact value depending on grain size and shear velocity[24]. The mean height to length ratio of typical saltation trajectories on Mars is 1:10 [24]. Saltation trajectories are generally asymmetrical such that the descending portion of the path (that which contains sand that hits the ground) occupies the greatest portion[45-47]. This should especially be the case for Mars where path lengths are longer than on Earth. Therefore, α should range from 0.1 to 0.2, with most trajectories toward lower values. Taking the average interdune sand flux (Q_i) of 2.3m^3 m^{-1} yr^{-1} (Earth year), values of z of 0.1 – 0.5m, and α ranging from 0.1 – 0.15 gives abrasion rates of 0.9 – 9μm yr^{-1} for a flat ground surface. For vertical rocks, the range is 9 – 46μm yr^{-1}. The field measurements in Victoria Valley, Antarctica[26] used samples elevated above the ground and sticking outward from an aluminum framework[48] and therefore closely represent that for vertical rock faces.

SOM Table 2: Dune migration speed and sand flux

Dune label	Height (m)	Migration rate (m yr^{-1})	Migration rate std. dev.	Sand flux (m^3 m^{-1} yr^{-1})	Sand flux std. dev.
1	38	0.07	0.01	2.66	0.38
2	15	0.27	0.08	4.05	1.20
3	29	0.05	0.01	1.45	0.29
4	22	0.17	0.03	3.74	0.66
5	31	0.09	0.02	2.79	0.62
6	24	0.13	0.03	3.12	0.72
7	20	0.07	0.02	1.40	0.40
8	30	0.05	0.01	1.50	0.30
9	21	0.20	0.05	4.20	1.05
10	24	0.05	0.01	1.20	0.24
11	16	0.09	0.02	1.44	0.32
12	25	0.03	0.01	0.75	0.25
13	12	0.05	0.02	0.60	0.24
14	39	0.09	0.02	3.51	0.78
a	9	0.12	0.12	1.08	1.08
b	13	0.12	0.12	1.56	1.56
c	10	0.12	0.12	1.20	1.20
d	17	0.12	0.12	2.04	2.04
e	40	0.12	0.12	4.80	4.80

f	38	0.12	0.12	4.56	4.56
g	15	0.12	0.12	1.80	1.80
h	22	0.12	0.12	2.64	2.64
i	20	0.12	0.12	2.40	2.40
j	16	0.12	0.12	1.92	1.92
k	12	0.12	0.12	1.44	1.44

SOM References

31. http://www.tectonics.caltech.edu/slip_history/spot_coseis/index.html

32. Avouac, J.P., F. Ayoub, S. Leprince, O. Konca, & D. Helmberger, The 2005, Mw 7.6 Kashmir earthquake, rupture kinematics from sub-pixel correlation of ASTER images and seismic waveforms analysis. *Earth Planet. Sci. Lett.* **249**, 514-528 (2006)

33. Necsoiu, M., S. *et al.* Monitoring Migration Rates of an Active Subarctic Dune Field Using Optical Imagery. *Rem. Sensing Envir.* **113**, 2441-2447 (2009)

34. http://webgis.wr.usgs.gov/pigwad/tutorials/socetset/SocetSet4HiRISE.htm

35. http://isis.astrogeology.usgs.gov/

36. http://www.socetgxp.com/content/products/socet-set

37. Kirk, R. *et al.* Ultrahigh resolution topographic mapping of Mars with HiRISE stereo images: Methods and first results. *7th International Conf. Mars*, 3381 Pasadena, CA (2007)

38. Mattson, S. Boyd, A., Kirk, R.L., Cook, D.A. & Howington-Kraus, E. HiJACK:

Correcting spacecraft jitter in HiRISE images of Mars. *European Planetary Science Congress*, EPSC2009-604 (2009)

39. Bookstein, F.L. "Principal Warps: Thin Plate Splines and the Decomposition of Deformations." *IEEE Trans. Pattern Anal. Mach. Intell. 11*, 567-585 (1989)

40. McEwen, A.S. *et al.,* Mars Reconnaissance Orbiter's High Resolution Imaging Science Experiment (HiRISE). *J. Geophys. Res.* **112**, doi:10.1029/2005JE002605 (2007)

41. http://naif.jpl.nasa.gov/naif/

42. Ashley, G.M. Classification of large-scale subaqueous bedforms – a new look at an old problem. *J. Sed. Petrology* **60**, 160-172 (1990)

43. Zimbelman, J.R. Transverse Aeolian Ridges on Mars: First results from HiRISE images. *Geomorph*. **121**, 22-29 (2010)

44. Simons, D.B. , Richardson, E.V., & Nordin, C.F. Bedload equation for ripples and dunes. U.S. Geological Survey Professional *Paper 462-H,* U.S. Gov. Printing Office, Washington, DC (1965)

45. White, B.R., & Schulz, J.C. Magnus effect in saltation. *J. Fluid Mech.* **81**, 497-512 (1977)

46. Greeley, R. & Iversen, J.D. *Wind As a Geological Process*, Cambridge University Press, New York (1985)

47. Bridges, N.T. *et al.*, Trajectories and energy transfer of saltating particles onto rock surfaces: Application to abrasion and ventifact formation on Earth and Mars. *J. Geophys. Res.* **110**, doi:10.1029/2004JE002388 (2005)

48. Malin, M.C. Preliminary abrasion rate observations in Victoria Valley, Antarctica.

Ant J. United States **18**, 25-26 (1984)